LAWRENCE
LIVERMORE
NATIONAL
LABORATORY

LLNL-TR-401214

A Proposal for First-Ever Measurement of Coherent Neutrino-Nucleus Scattering

C. D. Winant, A. Bernstein, M. P. Foxe, C. A. Hagmann, I. Jovanovic, K. M. Kazkaz, W. S. Stoeffl

February 11, 2008

Disclaimer

This work performed under the auspices of the U.S. Department of Energy by Lawrence Livermore National Laboratory under Contract DE-AC52-07NA27344.

FY07 LDRD Final Report
A Proposal for First-Ever Measurement of Coherent Neutrino-Nucleus Scattering
LDRD Project Tracking Code: 07-LW-062
C. Winant, Principal Investigator

Abstract

We propose to build and deploy a 10-kg dual-phase argon ionization detector for the detection of coherent neutrino-nucleus scattering, which is described by the reaction; $\nu + (Z,N) \rightarrow \nu + (Z,N)$, where ν is the scattering neutrino, and (Z,N) is the target nucleus of atomic number Z and neutron number N. Its detection would validate central tenets of the Standard Model. We have built a gas-phase argon ionization detector to determine the feasibility of measuring the small recoil energies (~ 1keV) predicted from coherent neutrino scattering, and to characterize the recoil spectrum of the argon nuclei induced by scattering from medium-energy neutrons. We present calibrations made with 55-Fe, a low-energy X-ray source, and report on measurements to date of the recoil spectra from the 2-MeV LINAC Li-target neutron source at LLNL. A high signal-to-noise measurement of the recoil spectrum will not only serve as an important milestone in achieving the sensitivity necessary for measuring coherent neutrino-nucleus scattering, but will break new scientific ground on its own.

Introduction/Background

Two-phase noble liquid/noble gas ionization detectors have enabled a new era of low-signal, low-background detection in non-accelerator-based particle physics. This versatile class of detectors can potentially be used to detect coherent neutrino scattering—an unmeasured prediction of the Standard Model of particle physics [1,2]. The existence of this process is also important in astrophysics, where coherent neutrino scattering is assumed to play an important role in energy transport within nascent neutron stars.

The potential scientific impact after discovery of coherent neutrino-nucleus scattering is large. This phenomenon is flavor-blind (equal cross-sections of interaction for all three neutrino types), lending the possibility that coherent scatter detectors could be used as total flux monitors in future neutrino oscillation experiments. Such a detector could also be used to measure the flavor-blind neutrino spectrum from the next nearby (d ~ 10kpc) type Ia supernova explosion. The predicted number of events [integrated over explosion time] for a proposed dual-phase argon coherent neutrino scattering detector is 10000 nuclear recoils/kton, compared to the estimated yield in the Solar Neutrino Observatory (neutral current configuration) of 200 deuteron breakup events/kton of D_2O [3,4].

In a more practical vein, these detectors may also be useful for improved cooperative monitoring of nuclear reactors, as required by the Nuclear Nonproliferation Treaty.

Recognizing this potential, the International Atomic Energy Agency, which administers the global reactor monitoring regime, has endorsed research into this technology.

Dual-phase liquid/gas noble element detectors have demonstrated exquisite sensitivity and background rejection in detecting low energy nuclear recoils, as evidenced in applications to direct dark matter detection [5,6] and neutrino-less double-beta decay [7]. We have proposed to build a 10 kg dual-phase liquid/gas argon detector for attempting a first-ever measurement of coherent neutrino-nucleus scatter.

Coherent Scatter Detection

The inverse beta-decay process $\nu_e + p \rightarrow n + e^+$ is commonly used to detect electron antineutrinos. By comparison, coherent antineutrino-nucleus scattering, $\nu + (Z,N) \rightarrow \nu + (Z,N)$, has a factor of N^2 higher interaction probability, where N is the number of neutrons in the target nucleus. This gain factor is what would allow for construction of high-rate, kilogram scale detectors.

Reactor antineutrinos ($E_\nu \sim 1$ MeV) interact coherently with the entire nucleus, with the resulting nuclear recoil ($E_r \sim 1$ keV) causing dE/dx ionization in the target medium. Our calculations have shown that these neutrinos will produce a maximum yield of 10 electrons per scatter recoil from an argon target. At a standoff distance of 25 m from the reactor core, ~200 detectable ionization events are expected per day in 10 kg of liquid argon [8]. Our Monte Carlo calculations show that argon has the largest number of antineutrino-induced ionization events of all noble gasses per unit of detector mass.

These weak ionization signals are detected when an electric field pulls the electrons through the liquid, across the gas-liquid boundary, and into an electroluminescence gap [9] that amplifies the signal and converts it into light. Each drift electron produces several hundred excited argon atoms along its track when subjected to an electric field strength of ~2-3 kV/cm across the gap. The de-excitation UV light is wavelength-shifted and detected by photomultiplier tubes.

The bulk of the detector backgrounds arise from radioactive contamination within and in the vicinity of the detector. Electrons from beta decay of ^{39}Ar and low-energy Compton electrons from background gammas will produce weak ionization events in the argon bath [10]. The contribution from the latter will be reduced with modest amounts of polyethylene and lead shielding around the detector [8] and the total background rate will be comparable to the neutrino signal rate. Since these aforementioned backgrounds are time-independent, they can be measured during periodic reactor shutdowns and subtracted.

A key element of the coherent scatter detection problem is to determine the detection threshold of a few-electron signal in a noble gas or liquid. Recent results from the XENON-10 collaboration in Italy indicate that a detection threshold of less than 4 primary electrons has been achieved in a dark matter detector prototype [5]. A second essential component of the research program is to experimentally measure the actual noise floor upon which this signal will lie, including noise sources such as sparking and corona discharge that are not captured in the Monte-Carlo simulations.

Another key element would be to measure the nuclear recoil quenching factor for both gas and liquid. The quenching factor is needed to meaningfully compare ionization signals induced respectively from electronic and nuclear scatters. The quenching factor

in liquid Argon has been published for nuclear recoil energies of 25 keV and above [11]. However, the quenching factor in argon liquid or gas has not been measured and reported in our energy range of interest (0.1 to 10 keV).

Once the signal and background measurements are accomplished with the dual phase detector, deployment at a reactor and measurement of the signal could proceed, made possible by the expected high interaction rate (hundreds of events per day). Aside from its intrinsic physical interest, measurement of coherent scatter can also enable practical applications of 10- to 50-liter-scale antineutrino detectors for reactor monitoring.

Work by other Researchers

Other researchers have been able to resolve X-ray peaks in the 10 - 30 primary electron range, corresponding to incident X-ray energies of several hundred electron-volts with Xenon-gas time projection chambers [12]. More recently, both the WARP collaboration in Italy and the XENON-10 collaboration have claimed detection thresholds of a 1-10 primary electron signal in a cryogenic dual-phase noble element ionization detector built for the purpose of dark matter detection [5,6].

The search for coherent neutrino-nucleus scatter is being pursued with other detectors. Both the TEXONO group [13] and the University of Chicago [14] are developing kilogram-scale high-purity Germanium detectors for the search. Studies are underway to measure coherent neutrino-nucleus scatter in a dual-phase argon detector with neutrinos from the Spallation Neutron Source at the Oak Ridge National Laboratory [15].

Method

We have built a single-phase argon gas detector as the first step in our coherent neutrino-nucleus recoil scatter measurement program. The detector consists of a flange-capped 35.5 cm by 30.4 cm-I.D. stainless steel cylindrical vessel into which gas is filled from commercially available cylinders. The chamber is evacuated by a dual stage turbo pump and diaphragm pump. The gas handling system is configured so that the chamber can be filled from two different gas cylinders, allowing for operation with gas mixtures.

Fig. 1: A photograph of the field cage for the Argon gas-phase detector, which is mounted on the inside of the top flange of the argon chamber. The field cage encloses an active argon volume of 10 cm by 10.2 cm I.D. Proportional scintillation is generated in the 4 cm by 10.2 cm I.D. volume above the active volume. A collimated 100 μCi 55-Fe X-ray source is installed below the drift region volume, generating free electrons that drift through the applied electric field convert to proportional scintillation between two fine-mesh grids. This light is the detected by a Hamamatsu H6410 5.1-cm diameter photomultiplier tube.

A two-stage high-voltage field cage is shown in Figure 1, and is mounted to the inside of the top flange of the vessel provides the electric fields necessary for drifting and for producing scintillation from collision-induced ionization in the argon. The field cage encloses an active argon volume of 10 cm by 10.2 cm I.D, (0.82 liter), henceforth referred to as the active volume, within the pressure chamber. Proportional scintillation is generated in the 4 cm by 10.2 cm I.D. volume (0.33 liter), henceforth referred to as the amplification volume, above the active volume. These two volumes are separated by a 1-mm pitch 30 μm-diameter gold-plated tungsten wire mesh. The scintillation generated in the amplification volume is detected through a 6.4 mm-thick quartz view-port by a 5.1 cm-diameter Hamamatsu H6410 fused-silica window photomultiplier tube operated at -2.6 kV bias. The electric fields of the active and amplification volumes are independently supplied by two 20-kV Bertan Series 225 high voltage power supplies. Ceramic-enclosed high voltage vacuum feed-throughs supply the high voltage into the chamber. One 375-MOhm axial resistor and six 75-MOhm axial resistors mounted in series across each aluminum ring of the field cage establish the respective electric fields in the active and amplification volumes. The field rings and meshes are mounted with insulating acrylic rods and spacers. A hemispherical aluminum cap and field-shaping rings surrounding each mesh minimize electric field gradients outside of the active volume, minimizing voltage-induced breakdown.
Raw signals from the photomultiplier tube are digitized and archived with a 2-channel 14-bit 200 MHz GaGe 14200 PC digitizer card. The digitizer interface facilitates triggering from a wide set of tuneable parameters, including voltage threshold, pulse width, pulse delay, or an external signal.

Detector Optimization

The scintillation signal detected by the photomultiplier tube is a measure of the collision-induced ionization yield from both nucleus and electronic recoils. The gain of this signal depends on many experimental details as well as both the energy of the recoiling particle and the quenching factor (in the case of nuclear recoils). These details include the mean free path of the drifting electron and the scintillation yield in the amplification region (which both depend on the electric field, the gas species and the gas density), the collection efficiency of the photomultiplier tube, the transmittance of the scintillation spectrum through the view-port and PMT window, and both the quantum efficiency and the electronic gain of the photomultiplier tube. A general course of optimization has been described in the dual-phase detector literature [9].

All measurements reported below were made at an operating pressure of 400 Torr, with a drift electric field of 0.4 kV/cm, and with an amplification electric field of 2 kV/cm. A small quantity of nitrogen gas (1.5 % of the total pressure) was introduced into the argon to boost the scintillation from the 120 nm characteristic emission of argon into the 300 to 400 nm band, which better matches the optical transmittance of the quartz view-port and the fused silica PMT window. This technique has been described in the literature [16].

The overall gain of the detector was first investigated by measuring the ionization spectrum created by a 100 μCi 55-Fe X-ray source with characteristic lines at 6 keV. The 55-Fe source was installed inside the field-shaping aluminum hemisphere, 1 cm below the active volume, with a collimated view into the active volume, and was present for all reported measurements. This ever-present signal guided the optimization of the parameters described above.

Measurements of neutron-induced nuclear recoils

Neutrons from a 2 MeV proton Li-target LINAC were used as a source of induced nuclear recoils in the argon gas detector [17]. The source generated 10^6 neutrons per second in the forward direction with an energy range of 10 to 100 keV (see Figure 2). We predicted that on order one neutron per spill would elastically scatter off an argon nucleus in the active volume. The known argon-neutron interaction cross section features a sharp resonance centered near 80 keV [18]. Incident neutrons within this 80-keV resonance were predicted to contribute to the bulk of the measured neutron-argon recoils.

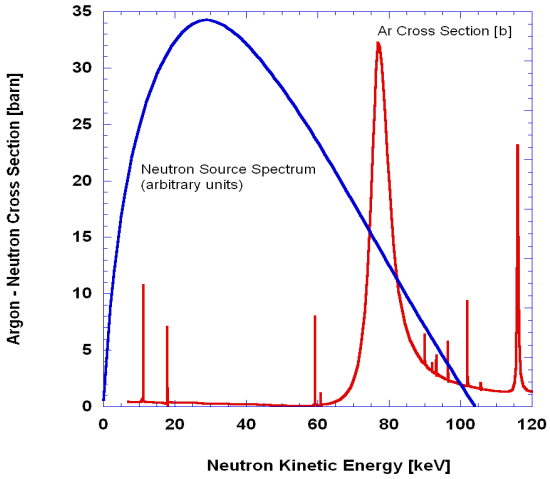

Fig. 2: The calculated neutron source spectrum of the LLNL 2-MeV LINAC Li-target neutron source (blue, arbitrary units) and the argon-neutron interaction cross section (red). The argon-neutron interaction cross section features a sharp resonance centered near 80 keV

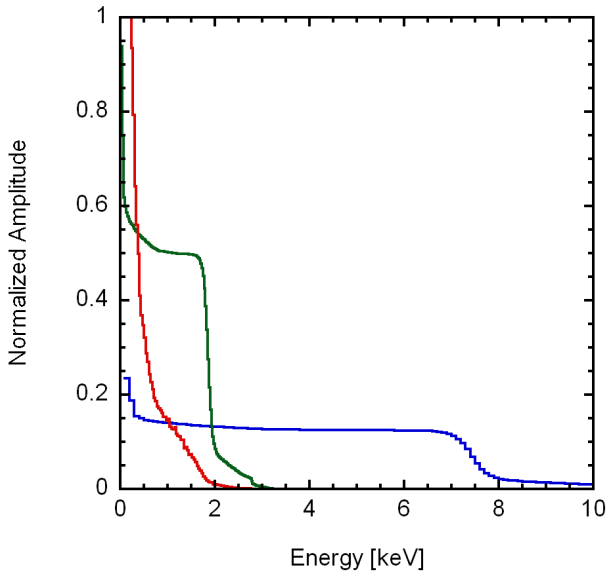

Fig. 3: The expected nuclear recoil spectrum induced by the incident neutron energy spectrum shown in Figure 2, (blue trace), the simulated electron-equivalent recoil spectrum, assuming a quenching factor of 0.25 (green), and the simulated scintillation spectrum measured by the photomultiplier tube

The nuclear recoil energy imparted by an 80 keV neutron is calculated to fall within the range of 0 to 8 keV, depending on the scatter angle. The expected nuclear recoil spectrum induced by the incident neutron energy spectrum, convolved with the interaction cross-section, is shown in Figure 3 (blue trace). The finite width of the resonance in the interaction cross-section contributes to the softened edge at the highest recoil energies. The simulated electron-equivalent recoil spectrum is shown in green. The two spectra differ by the quenching factor introduced in the previous section (a quenching factor of 0.25 was assumed for this simulation). The red curve in Figure 3 show the scintillation spectrum measured by the photomultiplier tube after incorporating the optical collection efficiency.

Experiments

For all measurements, the neutron source and argon detector were separated by a distance of one meter. The radio frequency quadrupole (RFQ) accelerator generated 30 μsec-wide periodic bursts of neutrons at a frequency of 100 Hz. The GaGe digitizer was triggered off the accompanying TTL pulse. The trace length was 200 μsec. The recorded waveforms were initialized 50 μsec before each trigger, and the neutron beam turned on 45 μsec after the TTL signal. The photomultiplier had an intrinsic transit response time of 2.6 ns. The analog photomultiplier signals were sampled at a rate of 5 ns / sample. Each measurement was acquired over 20 to 60 minutes.

The neutron source also generated 478-keV photons from (p,p'γ) interactions within the lithium target of the generator. These gammas were isotropically emitted from the target. Measurements were made in three different passive shielding configurations to separate signal contributions from source-correlated neutrons and gammas; (1) 5-cm lead (2) 12-cm borated polyethylene, and (3) no shielding. The transmission of the source neutrons and the gammas through both the lead and the borated polyethylene were calculated using MCNP Monte Carlo simulations, and were used to estimate the content of each beam for the three shielding configurations.

Results

Most waveforms contained anywhere from 0 to 10 distinct events, including both nuclear recoil candidates and background events. Background events included electronic recoils from 478 keV (p,p'γ) photons from the neutron generator, the 55-Fe X-rays, neutron-capture, decay, cosmic photons, single photoelectron noise events from the PMT, and scintillation discharge from high-voltage breakdown in the electric field cage. A thorough search of the data was made to identify and cut high-voltage breakdown events. All event identification and energy determination was performed with software on the raw waveforms.

Events from each waveform were separated into three time bins; those occurring before, during, and after the neutron beam. Energy spectra for each time bin were assembled from all the waveforms from a given measurement. The energy scale is obtained from the position of the 6-keV 55-Fe peak. The background energy spectra

were characterized from events within each trace acquired before the neutron beam was turned on.

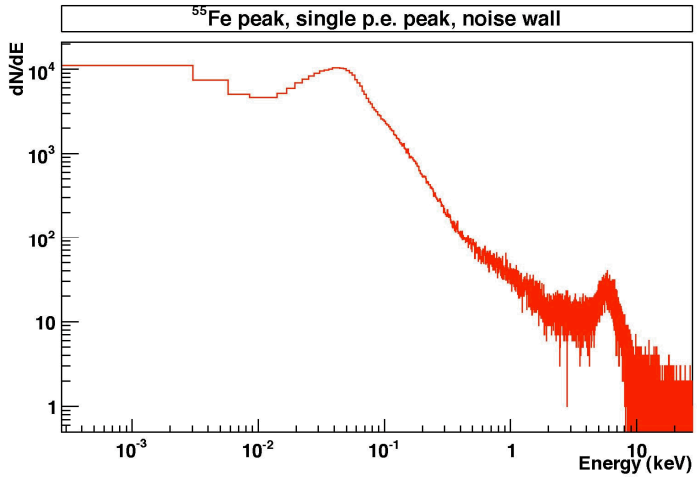

Fig. 4: Spectrum from 100 μCi 55-Fe source and background events, as measured in the Argon gas detector. The chamber pressure was 400 Torr. 1.5% nitrogen was introduced to enhance scintillation in the 300-400nm range. Electric fields of 0.4 kV/cm and 2 kV/cm were applied across the drift and amplification regions of the detector, respectively. The peak near 6 keV was produced by X-rays from the 55-Fe producing ~220 free electrons in the drift region of the detector.

Discussion and Conclusion

The data require further analysis before neutron-induced nuclear recoil spectra and the quenching factor for 8 keV nuclear recoils in argon can be quantified. Separating the photon component from the neutron component of the lead-attenuated data is the most involved step in the remaining analysis. We will attempt to separate these signals through comparisons of the data with different shielding materials and by making event cuts based on energy, time-width and time of arrival. These results are forthcoming. Next, we will build the dual-phase detector Upgrading from a gas to a liquid target will increase the target density by a factor of 800. The major tasks involved in upgrading from single (gas) phase to dual-phase are (1) refrigeration and temperature-control, (2) gas/liquid handling and purification, and (3) screening and selection of low-radioactivity background materials. We have designed the proposed dual-phase argon detector and are ready to begin building. Once the detector is built, time will be spent characterizing instrument-induced backgrounds. Internal radioactivity and high-voltage sparking mechanisms all contribute few-electron noise pulses that can swamp the expected neutrino signal. After characterizing backgrounds with both gas-phase and dual-phase detectors at LLNL, we will deploy the dual-phase detector in a gallery at 25 meters standoff from the core of the San Onofre Nuclear Generating Station (SONGS) in Southern California. The reactor provides a high flux source of antineutrinos for our investigation of coherent scatter, giving a rate of several hundred events per day in a 10 kg detector.

Acknowledgements

The authors are grateful to D. Dietrich and P. Kerr for providing the 2-MeV proton Li-target LINAC used in the experiments described in this paper.

References

[1] Freedman, D. Z. Phys. Rev. D9, 1389 (1974).
[2] Drukier, A., Stodolsky, L. Phys. Rev. D30, 2295 (1984).
[3] Waltham, C., in Proceedings of ICRC (2001), pp. 1189-1192, (Copernicus Gesellschaft, Germany).
[4] Horowitz, C. J., Coakley, K. J., and McKinsey, D. N. Phys. Rev. D68, 23005 (2003).
[5] Angle, J. *et al*. Submitted to Ap. J. (2007).
[6] Benetti, P. *et al*, in Proceedings of the 2006 XXII International Conference on Neutrino Physics and Astrophysics, Santa Fe, New Mexico, (unpublished).
[7] Danilov, M. Phys. Lett. B 480, 12 (2000).
[8] Hagmann, C. A. and Bernstein, A. IEEE Transactions on Nuclear Science, 51(5), 2151 (2004).
[9] Bolozdynya, A. Nucl. Instrum. Meth. A422, 314 (1999).
[10] Benetti, P. et al. Nucl. Instr. Meth. A Vol.574, Issue 1 (2007).
[11] Phipps, J. A., Boring, J. W., and Lewis, R. A. Phys. Rev. 135, A36 (1964).
[12] Borges, F. I. G. M. *et al*. Nucl. Instrum. Meth. A505, 242 (1999).
[13] Wong, H. *et al*. J.Phys.Conf., Ser. 39 (2006)
[14] Barbeau, P. S., Collar, J. I., and Tench, O. Journal of Cosmology and Astroparticle Physics, Issue 09, pp. 009 (2007).
[15] Scholberg, K. Phys. Rev. .D73,033005 (2006).
[16] Policarpo, A. J. P. L., Alves, M. A. F., and Conde, C. A. N. Nucl. Instrum. Meth. 55, 105 (1967).
[17] Dietrich, D. *et al*. Nucl. Instrum. Meth. B241, 826 (2005).
[18] Winters, R. *et al*. Phys. Rev. C43, 492 (1991).